# Formulating Brown Algae Derived Phloroglucinol-Based Epoxy Resin for High Performance Applications

Dyer, William E.; Gupta, Pranshul; Dransfeld, Clemens A.; Lorenz, Niklas; Kumru, Baris

**DOI**
10.1021/acsapm.4c02804

**Publication date**
2024

**Document Version**
Final published version

**Published in**
ACS Applied Polymer Materials

ACS APPLIED POLYMER MATERIALS



pubs.acs.org/acsapm

Article

# Formulating Brown Algae Derived Phloroglucinol-Based Epoxy Resin for High Performance Applications

William E. Dyer, Pranshul Gupta, Clemens A. Dransfeld, Niklas Lorenz, and Baris Kumru*

Cite This: https://doi.org/10.1021/acsapm.4c02804

Read Online

ACCESS | Metrics & More | Article Recommendations | Supporting Information

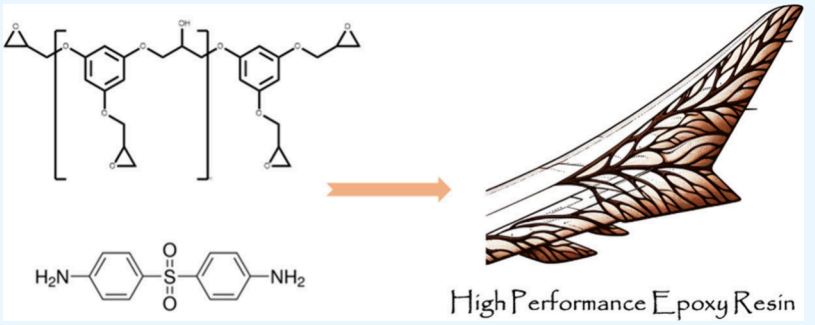


**ABSTRACT:** The development of epoxy resin formulations from renewable feedstocks has been thoroughly explored in the chemical literature. A simple one-pot chemical reaction involving sustainable phenolic molecules and epichlorohydrin results in the production of renewable epoxy monomers. These monomers can be cured with amines or anhydrides to yield cross-linked thermosetting resins. Although a wide variety of recipes exist, there is a notable gap in the application of these sustainable resin formulations to engineering contexts. This gap is primarily due to the lack of comprehensive, standardized analyses of these resin recipes, which impede their potential use in advanced composite applications. In this study, we reveal a high-performance resin formulation utilizing epoxidized phloroglucinol derived from brown algae in combination with an aerospace-grade amine hardener. The resin processing and thermomechanical properties are investigated using ASTM standard tests including tensile strength, flexural strength, fracture toughness, and interlaminar shear strength. Given the detailed comparative analysis, the partially renewable resin recipe outperforms petroleum derived analogues.

**KEYWORDS:** *renewable resin, sustainable epoxy, high performance resin, phloroglucinol epoxy, renewable composites*



## INTRODUCTION

Composite materials have significantly advanced the development of next-generation materials since the latter half of the 20th century, finding applications in aerospace, automotive, energy, and maritime industries.[1] These materials primarily consist of continuous glass or carbon fibers embedded in a polymer matrix, which can be either thermoplastic or thermoset.[2] The choice of matrix material is critical as it imparts many of the composite's unique properties and processability such as pultrusion,[3] thus necessitating careful selection based on end-use applications and desired characteristics. Thermoset matrices are diverse, including types such as bismaleimides, phthalonitriles, cyanate esters, vinyl esters, and epoxy resins.[4] Among these, epoxy matrices, typically cured with anhydride or amine hardeners, are the most prevalent; however other curing agents can be used.[5] The chemical structure and physical properties of the epoxy−hardener combination significantly influence cure kinetics, thermomechanical properties, and rheology, thereby impacting the composite manufacturing process and potential applications. For structural applications, carbon fibers are combined with high-performance resins having a high glass transition temperature ($T_g$), typically above 120 °C.[6] Epoxy resins with a $T_g$ ranging from 150 to 200 °C are suitable for use as primary and secondary aerospace resin systems.[7]

Despite the current efficacy of epoxy matrix materials, there are emerging concerns regarding their chemistry. Predominantly derived from petroleum, these materials are unsustainable and include chemicals like bisphenol A (BPA), a precursor to bisphenol A diglycidyl ether (BADGE), which is known to be an endocrine disruptor.[8,9] The synthesis of these compounds does not align with the green chemistry principle of utilizing renewable feedstocks.[10] Consequently, there is a growing need to explore renewable epoxy monomers as composite matrix materials. Natural $CO_2$ sequestering

Received: September 4, 2024
Revised: October 10, 2024
Accepted: October 10, 2024

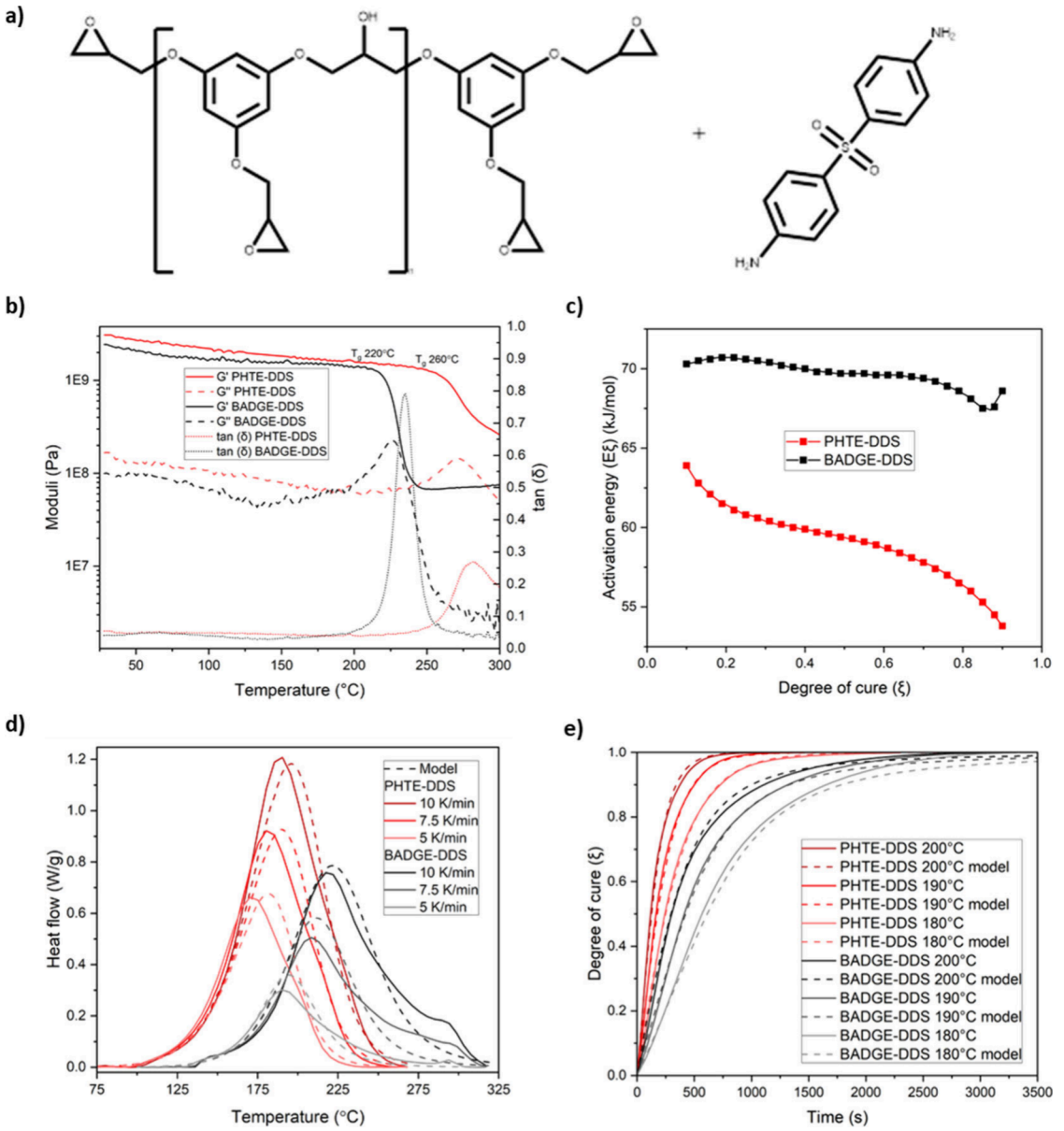


**Figure 1.** (a) Chemical structures of PHTE (left) and DDS (right). (b) DMA results for PHTE−DDS and BADGE−DDS. $T_g$ taken as onset of $G'$ decrease. (c) BADGE−DDS and PHTE−DDS activation energy development with degree of cure. (d) BADGE−DDS and PHTE−DDS nonisothermal data and model. (e) BADGE−DDS and PHTE−DDS isothermal data and model.

products such as plants and algae entail functional embodied carbon molecules that can be used in chemical industry.[11] Various renewable feedstocks have been investigated, including commercially available systems derived from cardanol and soybean.[12,13] However, these aliphatic and heterogeneous chemistries often result in thermomechanical properties that are unsuitable for high-performance composite matrices. Effective matrix materials must provide robust support for fibers across a broad temperature range and possess a relatively high $T_g$, making phenolic compounds attractive as potential BADGE alternatives as their aromatic nature contributes to advanced thermomechanical properties. The effect of aromaticity on generating high performance renewable resins has been illustrated by employing diverse renewable phenolics such as magnolol,[14] resveratrol,[15] eugenol,[16] and genistein.[17] However, the scalability of many phenolics remains a challenge. Additionally, the lack of standardized results in chemical literature complicates the assessment of renewable resins for composite applications.

Phloroglucinol is an aromatic alcohol extractable from brown algae in high yields.[18] Its synthesis is also being explored through various biosynthetic pathways, including genetically modified plants and bacteria.[19] Phloroglucinol triglycidyl ether (PHTE) has been investigated by Mija and colleagues, demonstrating good thermomechanical properties with an anhydride curing agent.[20] They also developed recyclable resins based on PHTE through precise chemical formulation stemming from on-demand degradable bonds.[21] Graillot and colleagues demonstrated an epoxidized vanillin and PHTE derived vitrimer resin formulation with outstanding reprocessability.[22] A renewable resin mixture based on epoxidized vanillin and PHTE generates a high performance thermosetting resin when cured with anhydrides with thermomechanical properties potentially addressing demands


https://doi.org/10.1021/acsapm.4c02804
ACS Appl. Polym. Mater. XXXX, XXX, XXX−XXX

for aerospace and naval sectors.[23] Our previous research revealed that a fast-curing resin system using PHTE with an aliphatic diamine hardener exhibited thermomechanical properties comparable to BADGE-based resins.[24] When using aliphatic diamine hardeners like Epikure 04998, the activation energy of the PHTE resin was significantly lower than that of the BADGE system, resulting in a renewable, fast-curing resin system. Despite fast-cure resin advantages, the thermomechanical properties of the resin were not qualified for structural engineering applications.

In this study, we assessed the suitability of PHTE for high-performance resin systems using the Huntsman Aradur 9664-1 hardener, a micronized 4,4′-diaminodiphenyl sulfone (DDS) commonly used in aerospace epoxy prepreg applications. The optimal mix ratio was identified, and the cure kinetics were studied. The thermal, physical, and mechanical properties of the resin system were evaluated using ASTM standards (D790, D638, D5045, D2765-16, D570, and D792) and compared to the analogous BADGE system.

## EXPERIMENTAL SECTION

**Materials.** Phloroglucinol tris epoxy (PHTE, epoxy content 8.3 mequiv/g, molecular weight 450 g/mol) was obtained from Specific Polymers. Bisphenol A diglycidyl ether (BADGE) monomer was obtained from Sigma-Aldrich. 4,4-Diaminodiphenyl sulfone (DDS, Aradur 9664-1) was obtained from Huntsman as a micronized powder. Unidirectional carbon fiber (200 g/m$^2$) was employed as reinforcing fiber for ILSS testing, obtained from R&G Faserverbundwerkstoffe GmbH. Marbocote 227, sealant type Cytec LTS90B/G, Wrightlon 8400 nylon film from Airtech, and Stich Ply A peel ply from MCTechnics were used for composite manufacturing. Details on sample preparation, analytical tools, specimen properties, and formulations to obtain mechanical properties are presented in Supporting Information with all details.

## RESULTS AND DISCUSSION

Materials and detailed experimental/analytical procedures are provided in the Supporting Information. Formulation of resin starts with identifying the correct mix ratio.[25] Although amine/epoxy equivalent weights allow for such calculations based on molecular structures, the presence of oligomers from the epoxidation reaction can affect the actual ratio.[26] DDS is a solid crystalline hardener with a melting point of 178 °C. When working with crystalline hardeners, the epoxy monomer can act as a solvent, enabling hardener dissolution before reaching its melting point and thus providing a larger processing window.[27] Mixing ratio studies involved using various ratios and analyzing the resin via dynamic mechanical analysis (DMA) to monitor temperature-dependent storage modulus and $T_g$ development (Figure S1). BADGE−DDS stoichiometry was provided by suppliers, resulting in a molar ratio of 2.06:1 for the BADGE−DDS system and 1.52:1 for the PHTE−DDS system (chemical structures of monomers are given in Figure 1a) corresponding to 2.82:1 and 1.80:1 mass ratios, respectively. The initial curing temperature is 180 °C for 2 h due to the melting point of DDS. Postcuring studies indicate that 220 °C postcuring is sufficient to achieve the highest $T_g$ of the PHTE−DDS system (Figure S2). The final $T_g$ as determined by DMA (Figure 1b) was 260 °C for PHTE−DDS and 220 °C for BADGE−DDS. As is well documented for epoxy−amine systems the curing temperature can be below the $T_g$ with the final $T_g^\infty$ exceeding the curing temperature.[28,29] Further DSC studies were performed to model the kinetics of the PHTE−DDS system and the BADGE−DDS system to compare the two. First, the activation energy ($E_\xi$)-dependency for heating rates of 2.5, 5, 7.5, and 10 K/min was evaluated from 0.1 to 0.9 within intervals of 0.01. Figure 1b shows $E_\xi$ calculated according to Supporting eqs 4 and 5 (SI section 1.3.1), mapping the evolution of activation energy for both systems as a function of degree of cure. The activation energy ranges from 65 to 52 kJ/mol for PHTE−DDS, which is located slightly above the activation energies of conventional epoxy−amine reactions, typically ranging from 20 to 60 kJ/mol. This is likely due to the aromatic nature of DDS, and the initial $E_a$ yields similar results as an epoxy resin cured with DDS, which exhibits initial $E_a$ of 64 kJ/mol.[30] At $\xi \approx 0.7$, the close-to-linear relation of activation energy and degree of cure decreases, and lower energies are required. The decrease in $E_a$ for PHTE−DDS could be due to the autocatalytic effect of hydroxyl groups on epoxy−amine reactions. PHTE has epoxy groups in much closer proximity than BADGE, which could lead to enhanced autocatalytic effect, which is especially relevant during latter stages of the reactions where secondary amine−epoxy reactions have a higher activation energy.[31,32] BADGE−DDS has higher $E_a$ of around 70 kJ/mol, which remains fairly consistent throughout the curing process.

The decrease in $E_a$ for PHTE−DDS indicates that the rate-determining step of curing changes from primary and secondary amine reactions to a process with a smaller activation energy, likely the autocatalytic hydroxyl mediated reaction. Because the contribution of this process increases with conversion, the value of $E_a$ at the end curing ($\xi = 0.9$) may be used to estimate the activation energy of the respective rate-determining processes. The resulting value (52 kJ/mol) might be attributable to the activation energy of the principal curing reactions such as autocatalyzed primary and secondary amine addition. However, this value is well above the activation energy of diffusion of small molecules (20 kJ/mol),[33] so an effect of vitrification can be excluded. As indicated in Figure 1c, the change of $E_\xi$ emphasizes that the cross-linking exhibits a more complex behavior and involves multiple reaction mechanisms that require supplementary investigation. Therefore, a model-based kinetic approach is selected to model the reaction kinetics.

Isothermal and dynamic DSC scans provide the basis for the multivariate analysis of six measurements at three different heating rates (5, 7.5, 10 K/min) and three isothermal curing temperatures (180, 190, 200 °C) (Figure 1d,e). The degree of cure through the tests was obtained using eq 1.

$$\xi = \frac{1}{H_{R,tot}} \int_0^t \left(\frac{dH}{dt}\right) dt \tag{1}$$

with $H_{R,tot}$ describing the total heat of reaction and $H$ describing the reaction. For the model-based kinetic modeling, the Kamal−Sourour phenomenological autocatalytic model of $m$th + $n$th order (eq 2) was selected for describing the reaction behavior of the reactive system:

$$\frac{d\xi}{dt} = (k_1 + k_2\xi^m)(1 - \xi)^n \tag{2}$$

$$k_i = A_i\, e^{-E_i/(RT)} \tag{3}$$

with $n$, $m$, $E_i$ and $A_i$ describing fitting parameters and $R$ being the molar gas constant. The six parameters of the reaction kinetic model are computed using a generic algorithm in Matlab, MathWorks Inc., USA. The differential equation (eq


https://doi.org/10.1021/acsapm.4c02804
ACS Appl. Polym. Mater. XXXX, XXX, XXX−XXX

2) is solved numerically by using an ode45-solver and initial condition $\xi = 0.01$.[34] The model parameters are concurrently identified for all data sets, resulting in an equal consideration of isothermal and nonisothermal curing conditions. The isothermal measurements are integrated into the fitting process, as they are essential for accurately simulating curing behavior under isothermal conditions.[35] Table 1 overviews the fitted parameters according to eqs 2 and 3.

**Table 1. Parameters for the Reaction Kinetic Modeling Revealed by Eqs 2 and 3**

| $m$ | $n$ | $A_1$ [log ($s^{-1}$)] | $E_1$ [kJ $mol^{-1}$] | $A_2$ [log ($s^{-1}$)] | $E_2$ [kJ $mol^{-1}$] |
|---|---|---|---|---|---|
| 1.02 | 1.07 | 3.63 | 54.42 | 7.28 | 86.54 |

Further, Figure 1d,e compares measured data and the proposed phenomenological model, showing a good agreement between modeling and experimental data. Through numerical integration of eq 2 with the identified parameters, the cure evolution can be determined for arbitrary curing cycles.

Rheology was used to characterize and compare the viscosity profile (Figure S3) and gel point of the two systems (Figure 2a). At 23 °C the BADGE−DDS system has an initial mix viscosity of 31.9 Pa·s, compared to 20500 Pa·s for the PHTE−DDS system (Figure S3).

At 100 °C, viscosities are 48.3 mPa·s for BADGE−DDS and 6550 mPa·s for PHTE−DDS, which potentially introduce composite manufacturing difficulties by means of resin impregnation, justifying the use of high injection pressures to ensure sufficient resin flow. The gel-point of the BADGE system at 120 °C is above 225 min compared to 65 min for the PHTE system (Figure 2a). This faster gel-time is due to the lower activation energy of PHTE−DDS reaction as shown by kinetic modeling, potentially due to the presence of more hydroxyl groups and therefore a faster rate of curing.

DMA was used to verify the postcuring temperature (Figure S2), verify stoichiometric ratios (Figure S1), and compare the viscoelastic behavior of PHTE−DDS and BADGE−DDS over a temperature range (Figure 1b). DMA showed a higher storage modulus at room temperature for PHTE−DDS of 3.08 GPa compared to 2.44 GPa for BADGE−DDS at room temperature. For BADGE−DDS this decreased to 67 MPa after the glass transition, but for PHTE−DDS the modulus was significantly higher after $T_g$ at 270 MPa due to the much higher cross-linking-density for the PHTE system due to its increased functionality compared to BADGE. This leads to a more rigid network, even above $T_g$. From these results the thermomechanical performance of the PHTE−DDS system seems higher than the BADGE−DDS system; however, both exhibit $T_g$ values above the application temperatures for structural composites. Hence, mechanical properties at room temperature bear significant importance for performance assessment.

The thermal stability of resin systems was analyzed by thermogravimetric analysis (TGA) at a heating rate of 10 °C/min (Figure 2b) showing $T_{onset}$ for the PHTE−DDS system at 290 °C in comparison to 330 °C for the BADGE−DDS system. However, at 500 °C, BADGE−DDS had lost 75% of its mass, compared to just 44% for PHTE−DDS, showing a slower thermal degradation process for the bio-based system. Evidently, a higher char yield at 900 °C of 24% for PHTE−DDS compared with 1.4% for BADGE−DDS was observed. Thermomechanical analysis (TMA) data (Figure 3a) showcases the dimensional changes of BADGE−DDS and PHTE−DDS. Using this data, one can calculate a coefficient of thermal expansion for both resin systems. PHTE−DDS has a coefficient of 97.75 × $10^{-6}$ $K^{-1}$, compared to 84.45 × $10^{-6}$ $K^{-1}$ for BADGE−DDS. This suggests that PHTE−DDS volumetrically expands slightly more than BADGE−DDS below $T_g$.

Water contact angles of both systems were measured for comparison to identify surface hydrophilicity (Figure S4). From the average of 5 samples (Table S1), we can see that both resins are hydrophilic due to the abundance of hydroxy units after curing. PHTE−DDS is more hydrophilic than BADGE−DDS, with an angle of 69° compared to 80° for BADGE, which could be ascribed to the higher aromaticity of the BADGE−DDS (aromatic/aliphatic atoms = 1.16:1 for BADGE−DDS and 0.76:1 for PHTE−DDS). Water absorption of the resin systems was studied via ASTM D570 (Tables S2 and S3). Across 3 days BADGE−DDS and PHTE−DDS showed similar levels of water absorption; however after 14 days the PHTE−DDS had absorbed almost 20% more water

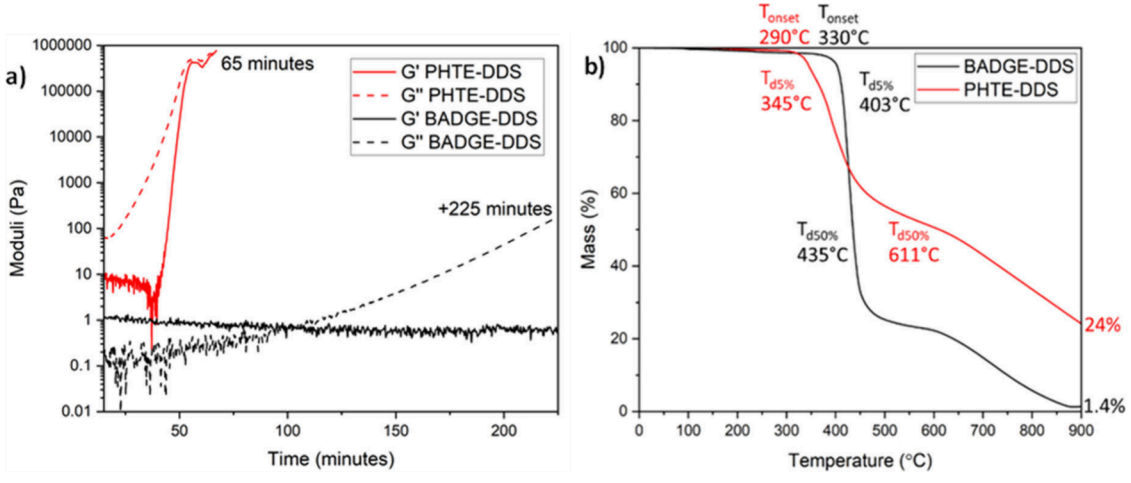


**Figure 2.** (a) Storage and loss modulus development of PHTE−DDS (red) and BADGE−DDS (black) systems at 120 °C showing a gel point of 65 min for PHTE−DDS and a gel point of BADGE−DDS far above 225 min at this temperature. (b) TGA of resin systems. Heating rate = 10 °C/min from 25 to 900 °C.


https://doi.org/10.1021/acsapm.4c02804
ACS Appl. Polym. Mater. XXXX, XXX, XXX−XXX

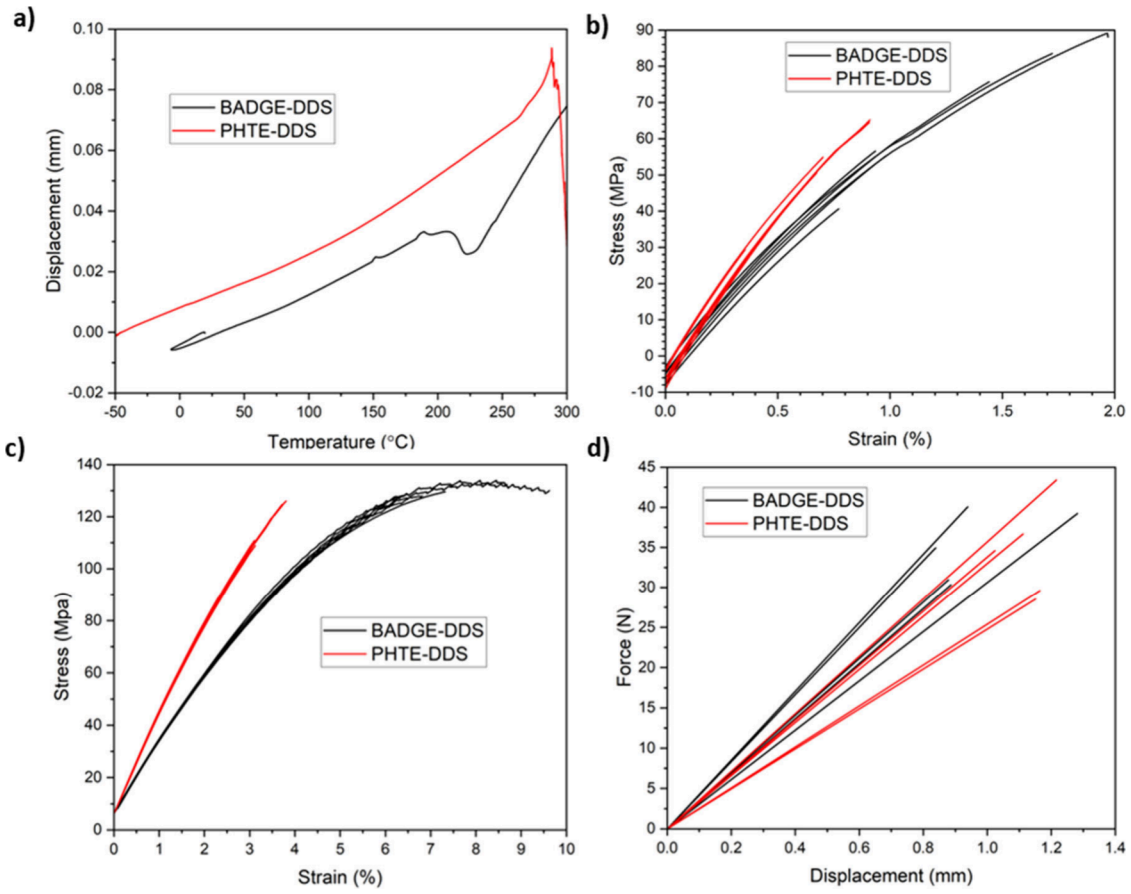


**Figure 3.** (a) Graph obtained from thermomechanical analyzer. (b) Tensile stress vs strain graph. (c) Flexural stress vs strain graph. (d) Force vs displacement graph from SENB samples. Sample dimensions have slight variation, leading to different $K_{IC}$ values even though some plots overlap.

**Table 2. Mechanical and Thermal Properties of the BADGE−DDS and PHTE−DDS Resins**

| resin system | $T_{g,DMA}$ [a,b] (°C) | $T_{d5\%}$, $T_{d50\%}$ (°C) | $\eta_{25°C}$, $\eta_{100°C}$ (Pa·s) | $\alpha$ ($K^{-1}$) | $G'_{25°C}$, $G'_{140°C}$ [c] (MPa) | flexural modulus [d] (GPa) | tensile modulus [e] (GPa) | tensile strength [e] (MPa) | fracture toughness ($K_{IC}$) [f] (MPa·m$^{1/2}$) |
|---|---|---|---|---|---|---|---|---|---|
| BADGE−DDS | 220 | 403, 435 | 31.9, 0.0483 | $84.45 \times 10^{-6}$ | 2.44, 1.56 | 2.60 | 1.20 | 83 | 0.51 |
| PHTE−DDS | 260 | 345, 611 | 20500, 6.55 | $97.75 \times 10^{-6}$ | 3.08, 1.88 | 3.77 | 1.79 | 67 | 0.99 |

[a] 5 °C/min heating rate. [b] Onset of $G'$ drop. [c] DMA. [d] ASTM-D790. [e] ASTM-D638. [f] ASTM-D5045.

than the BADGE−DDS sample. Gel content is a key parameter in assessing the degree of cure of a resin and is examined by ASTM D2765 (Table S4). Samples are submerged in hot toluene to dissolve any nongelled or microgelled parts of the resin. The remaining mass after 72 h can be termed the gel content. The gel content of postcured samples is very comparable almost at 100%, indicating fully reacted epoxy−amine constituents to form a continuous network. Resin density is an important parameter, which on large scale has direct influence on total composite weight and is especially critical in aerospace applications. ASTM D792 was used to calculate resin densities (Table S5 and S6), and an average density of 1.217 g/cm$^3$ for BADGE−DDS and 1.333 g/cm$^3$ for PHTE−DDS was determined. Higher density represents a drawback for the renewable resin system, which can be only compensated if mechanical properties are improved compared to petroleum counterparts.

Flexural, tensile, and fracture toughness (through single edge notch bending, SENB) mechanical tests were performed on both BADGE−DDS and PHTE−DDS specimens (Table S7−12) according to ASTM standards (D790, D638, and D5045, respectively; some examples are given in Figures S5−7). Sample preparation and verification steps are detailed in Supporting Information (section 1.4).

Tensile tests were performed using ASTM D638 to conduct a comprehensive comparison on the tensile strength and modulus. The tensile stress−strain graph is provided in Figure 3b, and results are presented in Table 2. The ultimate tensile strength of the PHTE−DDS resin is 67 MPa, that is 23% less than BADGE−DDS which has an ultimate tensile strength of 83 MPa. However, the Young's modulus of PHTE−DDS is 1.79 GPa which is considerably (33%) higher than that of BADGE−DDS (1.2 GPa). Overall, in tension properties PHTE−DDS is less ductile but stiffer compared to BADGE−DDS. Flexural testing was performed using ASTM D790 and the resulting stress−strain graph is given in Figure 3c. The modulus of elasticity in bending or flexural modulus is calculated as 3.77 GPa for PHTE−DDS which is 42.3% higher


https://doi.org/10.1021/acsapm.4c02804
ACS Appl. Polym. Mater. XXXX, XXX, XXX−XXX

as compared to 2.6 GPa for BADGE−DDS. The higher flexural modulus of a resin could be beneficial in some cases where it can resist buckling more effectively in a composite structure.

Following these mechanical tests, SENB testing was performed to obtain the value of material fracture toughness ($K_{IC}$). As previously seen, the PHTE−DDS resin offers significantly greater stiffness but lower strength than BADGE−DDS resin. This was also seen in the SENB testing in which the PHTE samples were subjected to higher loads before fracture occurred. $K_{IC}$, the plane strain fracture toughness, is a measure of the resistance of a material to crack extension under predominantly linear-elastic conditions. Higher $K_{IC}$ values indicate a greater ability to prevent fracture propagation in the material. As such, it is incredibly important in composite applications where the main failure modes arise from cracks propagating through the matrix, breaking the fibers, and leading to catastrophic failure of parts.[36] SENB postprocessing is highlighted in the SI (section 1.4.3). The fracture toughness can be taken as 0.99 MPa·m$^{1/2}$ for PHTE−DDS which is 48% higher as compared to 0.51 MPa·m$^{1/2}$ for BADGE−DDS. This could be due to the higher cross-link density or higher absolute density of PHTE−DDS. More connections to the stress point allow for more avenues for energy dissipation throughout the polymer network. Table 2 summarizes and compares the thermomechanical properties of so-formed resins in this work.

Interlaminar shear tests were performed on the composite laminates (Supplementary section 1.4.4, Figures S8 and 9, Tables S13−16). The ILSS results were 67.97 ± 6.51 MPa for PHTE−DDS compared to 52.53 ± 3.72 MPa for BADGE−DDS. These results suggest significantly more favorable fiber−matrix interactions in the PHTE−DDS formulation compared to BADGE−DDS. One reason for this could be the increased concentration of hydroxyl groups in the PHTE−DDS resin, which is known to contribute to fiber−matrix interactions.

## CONCLUSIONS

Phloroglucinol holds significant promise as a renewable feedstock, particularly as it can be sourced from brown algae. Epoxidized phloroglucinol provides a trifunctional epoxy monomer that, in this study, was combined with 4,4′-diaminodiphenyl sulfone (DDS) to mimic aerospace-grade formulations with 63% bio-based content. We observed that the viscosity of the PHTE resin system was substantially higher than that of the BADGE system (viscosity at 60 °C: PHTE−DDS 101 Pa·s vs BADGE−DDS 0.5 Pa·s). The gel-point at 180 °C is significantly faster for PHTE−DDS compared to BADGE−DDS, at 100 s vs 29 min, due to lower activation energy of PHTE−DDS resin and potentially due to the increased solubility of DDS in PHTE. Cured PHTE−DDS resin exhibits a significantly higher char yield at 900 °C (24% vs 1.3%). Additionally, the PHTE−DDS system shows a slight increase in water absorption and density compared to those of the BADGE−DDS system. Notably, the PHTE−DDS resin demonstrates superior glass transition temperature ($T_g$) values (260 °C vs 220 °C) and enhanced mechanical performance, as evidenced by ASTM standard tests, particularly in terms of flexural modulus, fracture toughness, and interlaminar shear strength (ILSS). At this stage, one can conclude that renewable resin can outperform petroleum derived resin in many critical aspects, considering structural engineering applications.

Despite the promising potential demonstrated in this study, future efforts should focus on reducing the viscosity of the resin system or exploring alternative impregnation and composite processing routes. Moreover, further research can investigate composite formation and conduct comprehensive studies to evaluate performance of the composites such as damage tolerance or fatigue behavior. Overall, the renewable PHTE-based resin exhibits substantial potential for composite applications and could play a pivotal role in advancing the sustainable composite industry and technologies.

## ASSOCIATED CONTENT

### Supporting Information

The Supporting Information is available free of charge at https://pubs.acs.org/doi/10.1021/acsapm.4c02804.

Details of sample preparation and mechanical tests, formulations used to calculate mechanical properties, contact angle, water absorption, and tables delineating specimen properties for mechanical tests (PDF)

## AUTHOR INFORMATION


### Corresponding Author

**Baris Kumru** − *Aerospace Structures & Materials Department, Faculty of Aerospace Engineering, Delft University of Technology, 2629 HS Delft, The Netherlands;* orcid.org/0000-0002-1203-4019; Email: b.kumru@tudelft.nl

### Authors

**William E. Dyer** − *Aerospace Structures & Materials Department, Faculty of Aerospace Engineering, Delft University of Technology, 2629 HS Delft, The Netherlands*

**Pranshul Gupta** − *Aerospace Structures & Materials Department, Faculty of Aerospace Engineering, Delft University of Technology, 2629 HS Delft, The Netherlands*

**Clemens A. Dransfeld** − *Aerospace Structures & Materials Department, Faculty of Aerospace Engineering, Delft University of Technology, 2629 HS Delft, The Netherlands*

**Niklas Lorenz** − *Aerospace Structures & Materials Department, Faculty of Aerospace Engineering, Delft University of Technology, 2629 HS Delft, The Netherlands*

Complete contact information is available at: https://pubs.acs.org/10.1021/acsapm.4c02804


### Notes

The authors declare no competing financial interest.

## ACKNOWLEDGMENTS

Authors acknowledge valuable support from ASM department and DASML technical staff. B.K., C.A.D., and N.L. appreciate the contribution from the National Growth Fund program NXTGEN HIGHTECH 01.

## REFERENCES


(1) Mesogitis, T. S.; Skordos, A. A.; Long, A. C. Uncertainty in the manufacturing of fibrous thermosetting composites: A review. *Compos. A: Appl. Sci. Manuf.* **2014**, *57*, 67−75.

(2) Yaghoubi, V.; Kumru, B. Retrosynthetic Life Cycle Assessment: A Short Perspective on the Sustainability of Integrating Thermoplastics and Artificial Intelligence Into Composite Systems. *Adv. Sustain. Syst.* **2024**, *8*, No. 2300543.

(3) Moghaddam, A.; Kumru, B.; Bergsma, O. K. Recyclable twin matrix composites. *Compos. Commun.* **2024**, *50*, No. 102010.

(4) Dyer, W. E.; Kumru, B. Polymers as Aerospace Structural Components: How to Reach Sustainability? *Macromol. Chem. Phys.* **2023**, *224*, No. 2300186.

(5) Walter, M.; Neubacher, M.; Fiedler, B. Using thermokinetic methods to enhance properties of epoxy resins with amino acids as biobased curing agents by achieving full crosslinking. *Sci. Rep.* **2024**, *14*, 4367.
(6) Soutis, C. Fibre reinforced composites in aircraft construction. *Prog. Aerosp. Sci.* **2005**, *41*, 143−151.
(7) Ramon, E.; Sguazzo, C.; Moreira, P. M. G. P. A Review of Recent Research on Bio-Based Epoxy Systems for Engineering Applications and Potentialities in the Aviation Sector. *Aerospace* **2018**, *5*, 110.
(8) Chen, M. Y.; Ike, M.; Fujita, M. Acute toxicity, mutagenicity, and estrogenicity of bisphenol-A and other bisphenols. *Environ. Toxicol.* **2002**, *17*, 80−86.
(9) Vandenberg, L. N.; Hauser, R.; Marcus, M.; Olea, N.; Welshons, W. V. Human exposure to bisphenol A (BPA). *Reprod. Toxicol.* **2007**, *24*, 139−177.
(10) Ganesh, K. N.; Zhang, D.; Miller, S. J.; Rossen, K.; Chirik, P. J.; Kozlowski, M. C.; Zimmerman, J. B.; Brooks, B. W.; Savage, P. E.; Allen, D. T.; Voutchkova-Kostal, A. M. Green Chemistry: A Framework for a Sustainable Future. *ACS Omega* **2021**, *6*, 16254−16258.
(11) Derradji, M.; Mehelli, O.; Liu, W.; Fantuzzi, N. Sustainable and Ecofriendly Chemical Design of High Performance Bio-Based Thermosets for Advanced Applications. *Front. Chem.* **2021**, *9*, No. 691117.
(12) Jaillet, F.; Darroman, E.; Ratsimihety, A.; Auvergne, R.; Boutevin, B.; Caillol, S. New biobased epoxy materials from cardanol. *Eur. J. Lipid Sci. Technol.* **2014**, *116*, 63−73.
(13) Kadam, A.; Pawar, M.; Yemul, O.; Thamke, V.; Kodam, K. Biodegradable biobased epoxy resin from karanja oil. *Polymer* **2015**, *72*, 82−92.
(14) Cao, Q.; Weng, Z.; Qi, Y.; Li, J.; Liu, W.; Liu, C.; Zhang, S.; Wei, Z.; Chen, Y.; Jian, X. Achieving higher performances without an external curing agent in natural magnolol-based epoxy resin. *Chin. Chem. Lett.* **2022**, *33*, 2195−2199.
(15) Yang, H.; Yuan, G.; Jiao, E.; Wang, K.; Diao, W.; Li, Z.; Liu, Z.; Wu, K.; Shi, J. Resveratrol-Derived Liquid Crystal Epoxy Resin with Low-Dielectric Properties and Excellent Mechanical Strength and Toughness. *ACS Appl. Polym. Mater.* **2024**, *6*, 1116−1128.
(16) Wan, J.; Zhao, J.; Gan, B.; Li, C.; Molina-Aldareguia, J.; Zhao, Y.; Pan, Y.-T.; Wang, D.-Y. Ultrastiff Biobased Epoxy Resin with High Tg and Low Permittivity: From Synthesis to Properties. *ACS Sustainable Chem. Eng.* **2016**, *4*, 2869−2880.
(17) Dai, J.; Teng, N.; Liu, J.; Feng, J.; Zhu, J.; Liu, X. Synthesis of bio-based fire-resistant epoxy without addition of flame retardant elements. *Compos. B: Eng.* **2019**, *179*, No. 107523.
(18) Li, Y.; Fu, X.; Duan, D.; Liu, X.; Xu, J.; Gao, X. Extraction and Identification of Phlorotannins from the Brown Alga, Sargassum fusiforme (Harvey) Setchell. *Mar. Drugs* **2017**, *15*, 49.
(19) Meyer, A.; Saaem, I.; Silverman, A.; Varaljay, V. A.; Mickol, R.; Blum, S.; Tobias, A. V.; Schwalm, N. D.; Mojadedi, W.; Onderko, E.; Bristol, C.; Liu, S. T.; Pratt, K.; Casini, A.; Eluere, R.; Moser, F.; Drake, C.; Gupta, M.; Kelley-Loughnane, N.; Lucks, J. P.; Akingbade, K. L.; Lux, M. P.; Glaven, S.; Crookes-Goodson, W.; Jewett, M. C.; Gordon, D. B.; Voigt, C. A. Organism Engineering for the Bioproduction of the Triaminotrinitrobenzene (TATB) Precursor Phloroglucinol (PG). *ACS Synth. Biol.* **2019**, *8*, 2746−2755.
(20) Dinu, R.; Lafont, U.; Damiano, O.; Orange, F.; Mija, A. Recyclable, Repairable, and Fire-Resistant High-Performance Carbon Fiber Biobased Epoxy. *ACS Appl. Polym. Mater.* **2023**, *5*, 2542−2552.
(21) Dinu, R.; Lafont, U.; Damiano, O.; Mija, A. Sustainable and recyclable thermosets with performances for high technology sectors. An environmental friendly alternative to toxic derivatives. *Front. Mater.* **2023**, *10*, No. 1242507.
(22) Genua, A.; Montes, S.; Azcune, I.; Rekondo, A.; Malburet, S.; Dayde-Cazals, B.; Graillot, A. Build-To-Specification Vanillin and Phloroglucinol Derived Biobased Epoxy-Amine Vitrimers. *Polymers* **2020**, *12*, 2645.
(23) Dinu, R.; Lafont, U.; Damiano, O.; Mija, A. High Glass Transition Materials from Sustainable Epoxy Resins with Potential Applications in the Aerospace and Space Sectors. *ACS Appl. Polym. Mater.* **2022**, *4*, 3636−3646.
(24) Apostolidis, D.; Dyer, W. E.; Dransfeld, C. A.; Kumru, B. An algae-derived partially renewable epoxy resin formulation for glass fibre-reinforced sustainable polymer composites. *RSC Appl. Polym.* **2024**, *2*, 149−154.
(25) Dlugaj, A. M.; Arrabiyeh, P. A.; Eckrich, M.; May, D. Dual-Curable Epoxy-Amine Thermosets: Influence of Stoichiometry and Ratio between Hardeners on Thermal and Thermomechanical Properties. *ACS Appl. Polym. Mater.* **2024**, *6*, 2902−2912.
(26) Gonzalez, F.; Ortiz, P.; Galego, N. Oligomerization of phenylglycidylether. *Polym. Int.* **1997**, *42*, 163−168.
(27) Hu, B.; Wang, J.; Chen, X.; Wang, J. S.; Yang, S.; Zhu, L.; Zou, L. N.; Huo, S. Q. A fire-safe, single-component epoxy resin based on a phosphorus/imidazole-containing latent curing agent and diphenylphosphine. *Polym. Adv. Technol.* **2024**, *35*, No. e6238.
(28) Michel, M.; Ferrier, E. Effect of curing temperature conditions on glass transition temperature values of epoxy polymer used for wet lay-up applications. *Constr. Build. Mater.* **2020**, *231*, No. 117206.
(29) Studer, J.; Dransfeld, C.; Masania, K. An analytical model for B-stage joining and co-curing of carbon fibre epoxy composites. *Compos. - A: Appl. Sci. Manuf.* **2016**, *87*, 282−289.
(30) Hao, W.; Hu, J.; Chen, L.; Zhang, J.; Xing, L.; Yang, W. Isoconversional analysis of non-isothermal curing process of epoxy resin/epoxide polyhedral oligomeric silsesquioxane composites. *Polym. Test.* **2011**, *30*, 349−355.
(31) Chiao, L. Mechanistic reaction kinetics of 4,4′-diaminodiphenyl, sulfone cured tetraglycidyl-4,4′-diaminodiphenylmethane epoxy resins. *Macromolecules* **1990**, *23*, 1286−1290.
(32) Sbirrazzuoli, N.; Mititelu-Mija, A.; Vincent, L.; Alzina, C. Isoconversional kinetic analysis of stoichiometric and off-stoichiometric epoxy-amine cures. *Thermochim. Acta* **2006**, *447*, 167−177.
(33) Sbirrazzuoli, N.; Vyazovkin, S.; Mititelu, A.; Sladic, C.; Vincent, L. A Study of Epoxy-Amine Cure Kinetics by Combining Isoconversional Analysis with Temperature Modulated DSC and Dynamic Rheometry. *Macromol. Chem. Phys.* **2003**, *204*, 1815−1821.
(34) Anagwu, F. I.; Skordos, A. A. Cure kinetics, glass transition advancement and chemo-rheological modelling of an epoxy vitrimer based on disulphide metathesis. *Polymer* **2023**, *288*, No. 126427.
(35) Bernath, A.; Kaerger, L.; Henning, F. Accurate Cure Modeling for Isothermal Processing of Fast Curing Epoxy Resins. *Polymers* **2016**, *8*, 390.
(36) Cugnoni, J.; Amacher, R.; Kohler, S.; Brunner, J.; Kramer, E.; Dransfeld, C.; Smith, W.; Scobbie, K.; Sorensen, L.; Botsis, J. Towards aerospace grade thin-ply composites: Effect of ply thickness, fibre, matrix and interlayer toughening on strength and damage tolerance. *Compos. Sci. Technol.* **2018**, *168*, 467−477.


https://doi.org/10.1021/acsapm.4c02804
ACS Appl. Polym. Mater. XXXX, XXX, XXX−XXX